Synoptic-Scale Flow and Valley Cold Pool Evolution in the Western United States

HEATHER DAWN REEVES AND DAVID J. STENSRUD

NOAA/National Severe Storms Laboratory, Norman, Oklahoma

(Manuscript received 26 November 2008, in final form 11 June 2009)

ABSTRACT

Valley cold pools (VCPs), which are trapped, cold layers of air at the bottoms of basins or valleys, pose a significant problem for forecasters because they can lead to several forms of difficult-to-forecast and hazardous weather such as fog, freezing rain, or poor air quality. Numerical models have historically failed to routinely provide accurate guidance on the formation and demise of VCPs, making the forecast problem more challenging. In some case studies of persistent wintertime VCPs, there is a connection between the movement of upper-level waves and the timing of VCP formation and decay. Herein, a 3-yr climatology of persistent wintertime VCPs for five valleys and basins in the western United States is performed to see how often VCP formation and decay coincides with synoptic-scale (~200–2000 km) wave motions. Valley cold pools are found to form most frequently as an upper-level ridge approaches the western United States and in response to strong midlevel warming. The VCPs usually last as long as the ridge is over the area and usually only end when a trough, and its associated midlevel cooling, move over the western United States. In fact, VCP strength appears to be almost entirely dictated by midlevel temperature changes, which suggests large-scale forcing is dominant for this type of VCP most of the time.

1. Introduction

Orographic trapping of cold air in valleys and basins is a frequent occurrence during winter in the western United States. These valley cold pools (VCPs), as they are referred to herein, are defined as ''topographically confined, stagnant'' layers of air that are ''colder than the air above'' (Whiteman et al. 2001, p. 77). There are no formally accepted criteria used to identify VCPs, but they are usually described as having strong static stability (either a temperature inversion or a statically stable layer) and weak low-level winds that are decoupled in both speed and direction from the free atmosphere (e.g., Wolyn and McKee 1989; Whiteman et al. 2001; Billings et al. 2006).

There are two types of VCPs: diurnal and persistent. The diurnal variety forms as nocturnally cooled air drains to the bottom of the basin or valley and dissipates from insolation during the day (e.g., Lenschow et al. 1979; Banta and Cotton 1981; Whiteman 1982; Whiteman and McKee 1982; Bader and McKee 1985; Vrhovec 1991; Fast et al. 1996). Persistent VCPs are those that last longer than one diurnal cycle. This type of VCP can lead to some forms of hazardous and difficult-to-forecast weather including freezing rain, fog, and poor air quality (e.g., Hill 1993; Smith et al. 1997; Pataki et al. 2005; Struthwolf 2005). Hence, forecasters faced with a VCP are keenly interested in knowing the evolution of the thermodynamic properties of the VCP and how long it will last. Yet, historically persistent VCP temperature evolution has been difficult to anticipate (Smith et al. 1997). This may be partially due to the tendency for numerical models to remove VCPs too early and overpredict low-level temperatures (Zängl 2002; Hart et al. 2004, 2005; Reeves and Lin 2006; Cheng and Steenburgh 2007).

Climatological studies of persistent, wintertime VCPs show they are most common in midwinter and sometimes occur simultaneously in multiple basins and valleys (Wolyn and McKee 1989; Whiteman et al. 1999, 2001; Savoie and McKee 1995; Mayr and McKee 1995). Their average duration is typically between 1 and 2 days, but events lasting as long as 8 days have been documented (Wolyn and McKee 1989). This suggests that processes besides radiation play a role in maintaining VCPs. Wolyn and McKee (1989) and Whiteman et al. (1999) also found that VCP strength can fluctuate,

Corresponding author address: Heather Dawn Reeves, DOC/NOAA/OAR/National Severe Storms Laboratory, 120 David L. Boren Blvd., Ste. 2401, Norman, OK 73072-7319.
E-mail: heather.reeves@noaa.gov

DOI: 10.1175/2009WAF2222234.1

sometimes leading to a short period of time when the VCP criteria used are not strictly met, but the general weather conditions consistent with a VCP still exist. These partial mix outs are attributed to slight adjustments of the synoptic-scale (~200–2000 km) flow.

Some idealized experiments of persistent VCPs have been conducted. These focus primarily on decay mechanisms and, in particular, the effects of shear-induced mixing. The results from these studies are conflicting. Petkovsek (1992), Vrhovec and Hrabar (1996), and Zängl (2005b) found that shear-induced mixing can be an important removal mechanism while Lee et al. (1989) found it has little effect. Lee et al. (1989) and Zängl (2003) also considered the effects of changes in the large-scale pressure gradient and found that VCP removal is expedited when the pressure gradient is oriented so as to direct flow through openings in the valley or basin sidewalls. Finally, Zängl (2005a) considered the effects of radiation and drying on VCP formation and found a rather high amount of nocturnal cooling is required, suggesting that drying is an additional important maintenance mechanism.

Some observational studies of persistent VCPs have been performed. In many of these cases, a similar progression of synoptic-scale flows is described. Some authors note the VCPs are preceded by a low-level cold-air surge (Wolyn and McKee 1989; Whiteman et al. 1999, 2001; Zhong et al. 2001; Zängl 2005b). Wolyn and McKee (1989) suggest the surge may be the source for cold air later in the VCP life. Strong midlevel warm-air advection in association with an approaching upper-level ridge has been observed at VCP onset, most of these VCPs last as long as the ridge remains over the valley or basin, and end with the approach of an upper-level trough (Wolyn and McKee 1989; Whiteman et al. 1999, 2001; Zhong et al. 2001; Zängl 2005b; Hoggarth et al. 2006). In many of these studies, the authors attribute VCP formation and decay to the movement of the upper-level waves. This connection between synoptic-scale wave motions and VCP evolution may prove extremely useful for forecasting as synoptic-scale patterns are usually fairly well handled in numerical weather prediction models. There is evidence, though, that indicates some persistent wintertime VCPs may be primarily caused (or strongly enhanced) by radiational cooling and that VCP duration is increased when there is low-level cloud cover and fog, snow cover, or subcloud evaporation (Wolyn and McKee 1989; Whiteman et al. 1999, 2001; Zhong et al. 2001; Billings et al. 2006; Hoggarth et al. 2006) and it is not known whether the timing of VCPs is primarily dictated by synoptic-scale forcing for a larger collection of cases with a wider array of valley and basin sizes and geometries.

The aim of this paper is to perform a short-term climatology of persistent VCPs in valleys and basins of differing size, location, and geometry in the western United States to assess the connection between synoptic-scale wave motion and VCP formation, maintenance, and demise. The criteria used to identify VCPs, the valleys and basins considered, and the number of VCP occurrences are discussed in section 2. The VCPs are partitioned as episodic (times when VCPs occur simultaneously or nearly simultaneously at multiple locations) and nonepisodic (times when only one or two locations have a VCP). Episodic VCPs are presented and their synoptic-scale flow patterns are discussed in section 3. Nonepisode VCPs and episodes with missing VCPs are discussed in section 4. Conclusions are provided in section 5.

2. Valley cold pool identification and incidences

Persistent VCPs are identified using 12-hourly radiosonde data at five valley and basin locations in the western United States (Fig. 1). The sounding locations are at Spokane, Washington (OTX), which is in the Columbia River basin; Boise, Idaho (BOI), which is in the Snake River Valley; Salt Lake City, Utah (SLC), which is in the Bonneville Basin; Grand Junction, Colorado (GJT), which is in the Grand Valley of Colorado; and Reno, Nevada (REV), which is in the Lake Lohantan basin. Note that these basins and valleys represent a wide array of sizes, orientations, and locations. A VCP is identified when a sounding has an inversion below the maximum crest height of the surrounding mountains and average wind speeds beneath the inversion top that are less than 5 m s^{-1}. The maximum crest height is determined using the U.S. Geological Survey 30-s terrain-elevation dataset. These heights are 3.1 km for the Columbia River basin, 2.7 km for the Snake River valley, 3.4 km for the Bonneville Basin, 2.9 km for the Grand Valley, and 2.4 km for the Lake Lohantan basin. A persistent VCP is defined as having three or more consecutive 12-hourly soundings with a VCP. Persistent VCP occurrences for winter seasons from October 2005 to March 2008 are considered.

A timeline of VCPs over the study period is provided in Fig. 2. Notice that each location experiences a similar number of VCPs during the time considered and that most VCPs occur simultaneously or nearly simultaneously in multiple valleys and basins regardless of the size or location of the valley or basin. An example is the set of VCPs that occur from about 20 to 25 November 2005 when there are cold pools at all locations. We refer to groupings of three or more simultaneous or nearly simultaneous occurrences of cold pools as episodes.

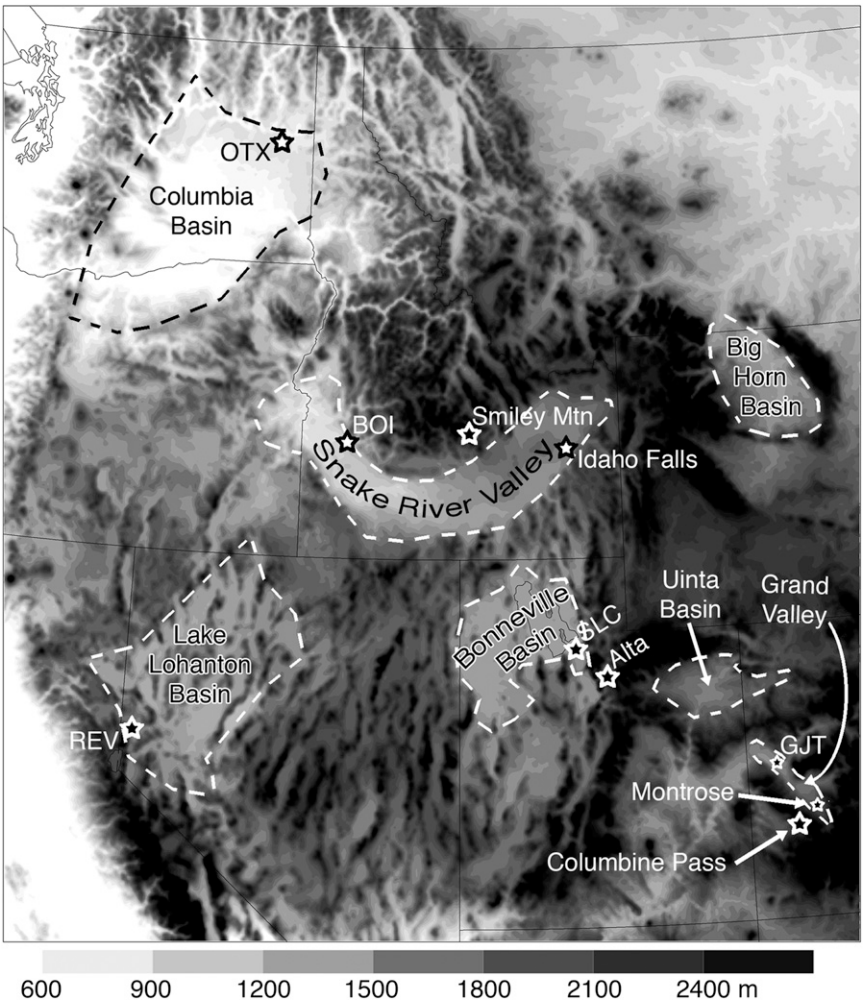

FIG. 1. The terrain height of the western United States (shaded). The locations of valleys and basins referred to in the text are indicated as are locations of radiosondes and select surface observation sites.

During the time period considered, there are 29 episodes and 53 nonepisodes. The nonepisodic VCPs are typically of a much shorter duration than are the episodes and are more prone to occur relatively early or late in the season rather than in midwinter.

The proclivity for VCPs to occur in multiple locations rather than as isolated incidents suggests larger-scale processes are important for forming, maintaining, and ending persistent VCPs, regardless of the valley or basin size, most of the time. In the following section, we investigate the evolution of episodic VCPs and their attendant synoptic-scale flow patterns. Throughout this paper, we will refer to different times in the VCP life cycle. These are before episode onset (which is taken to be 24 h before the start of an episode), at the episode start (which is given by the start of the areas of gray shading in Fig. 2), the episode end (which is given by the end of areas of gray shading in Fig. 2), the episode middle (which is the midpoint between the start and end), and after the episode ends (which is taken to be 24 h after the end of an episode).

3. Episodic valley cold pools

a. VCP evolution

A composite analysis of observed vertical temperature profiles at different times in the life cycle of episodic VCPs shows all locations have a similar temperature evolution, regardless of the size or orientation of the valley or basin in which they are located (Fig. 3).[1] Before

[1] No correction for diurnal effects and the different times of day the episodes start, are at their midpoints, or end are made in these, or any other, composites.

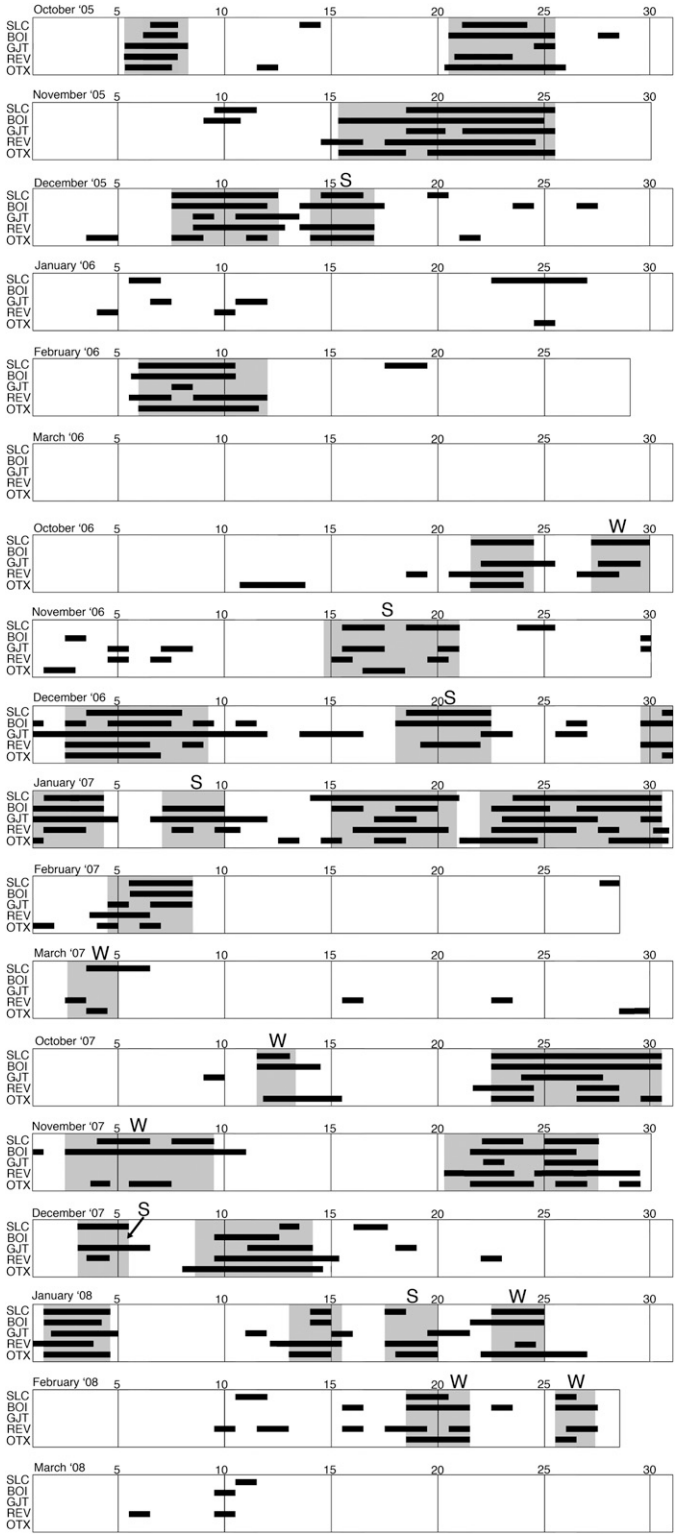

FIG. 2. A timeline of persistent cold pools for five basins and valleys in the western United States. The gray shading denotes episodes when three or more basins and valleys simultaneously or nearly simultaneously have cold pools. The ''W'' and ''S'' denote episodes that are weak and strong, respectively (see section 4).

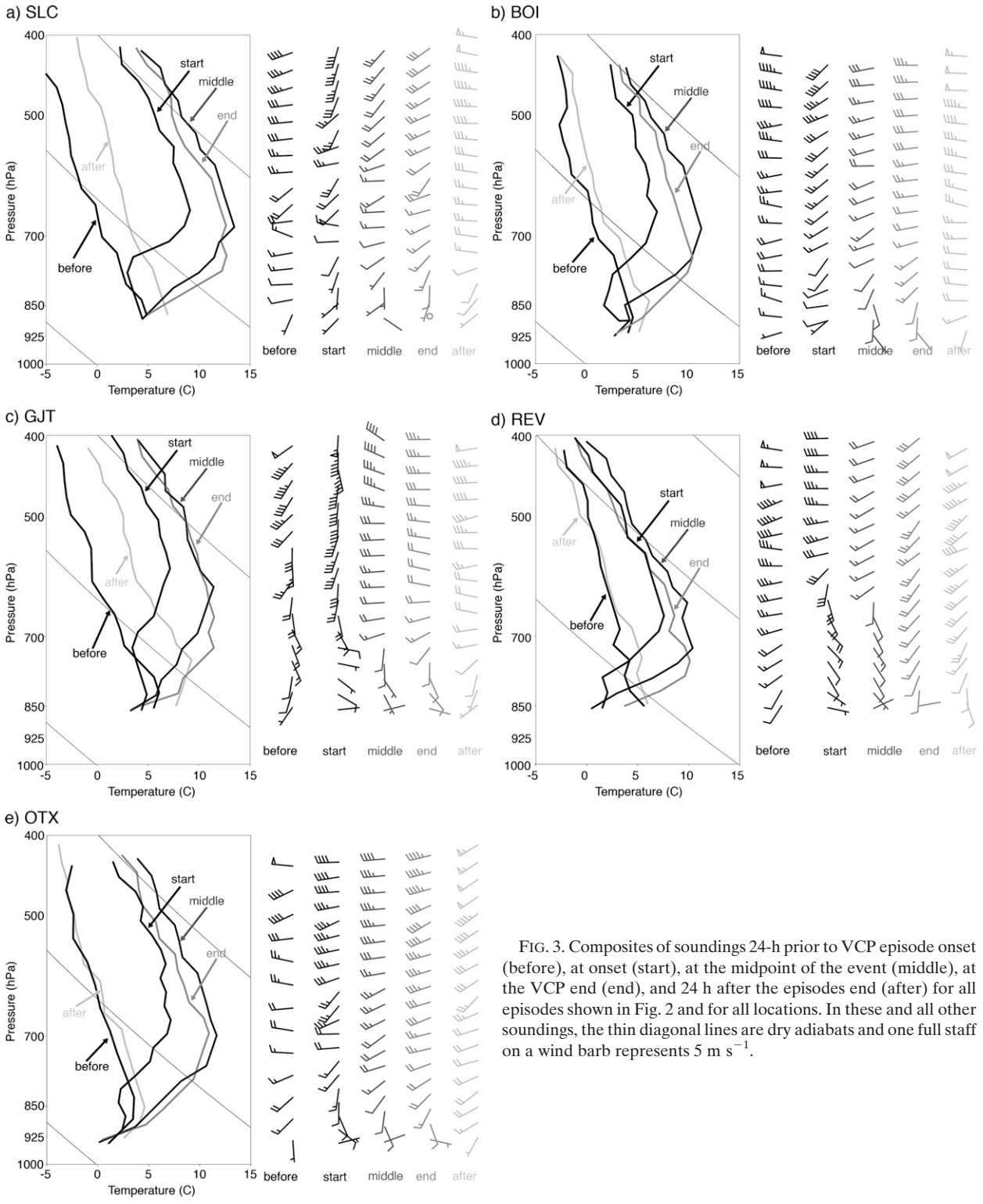

FIG. 3. Composites of soundings 24-h prior to VCP episode onset (before), at onset (start), at the midpoint of the event (middle), at the VCP end (end), and 24 h after the episodes end (after) for all episodes shown in Fig. 2 and for all locations. In these and all other soundings, the thin diagonal lines are dry adiabats and one full staff on a wind barb represents 5 m s^{-1}.

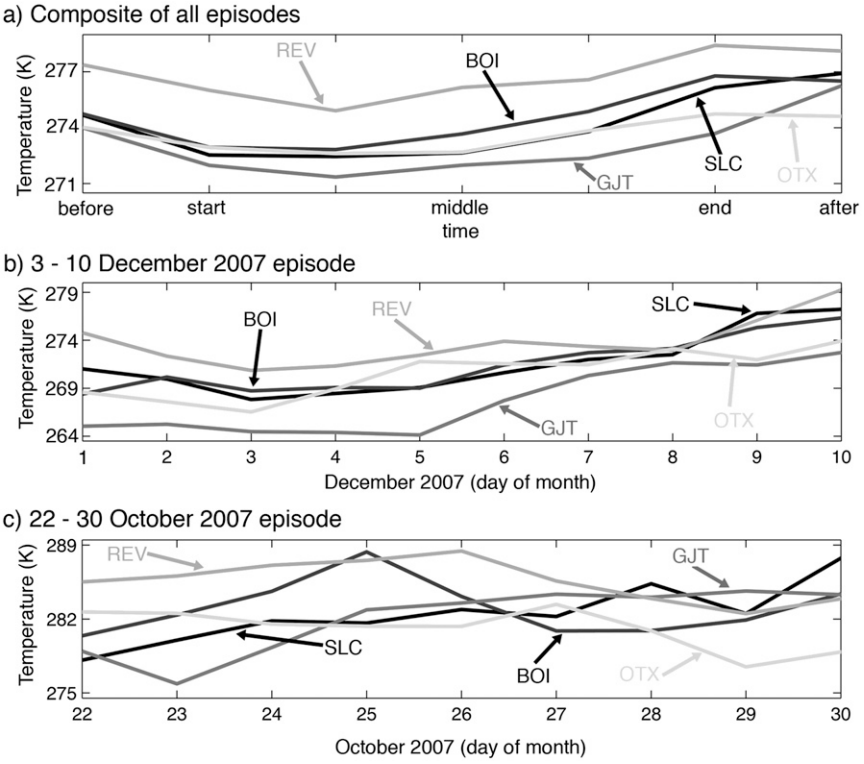

FIG. 4. Meteograms of observed (a) composites of 2-m temperature at key times in the VCP life cycle (this includes one-quarter and three-quarters of the way through the episodes) and (b),(c) daily mean 2-m temperatures for two VCP episodes. In (b),(c), the day markers indicate 0000 UTC of the day given.

the episode onset, the temperature profile is usually nearly moist neutral. The onset is marked by strong midlevel (700–500 hPa) warming. Between episode starts and ends, the bases of the inversions descend and there is additional midlevel warming. Episodes end with strong midlevel cooling. These large changes in the midlevel temperature at the beginnings and ends of the episodes support the notion that synoptic-scale flow patterns drive the formation and decay of episodic VCPs most of the time. Conversely, the temperature profiles in the lowest 100 hPa often initially have weak cooling followed by a warming of the near-surface layer toward the end of the event, an evolution that suggests diurnal cooling typically plays only a secondary role in forming and maintaining persistent VCPs.

The progression patterns of the mid- and upper-level (above 700 mb) wind directions in Fig. 3 are also similar at all locations. The winds generally are from the southwest or south at VCP onset and transition to a west or southwest direction as the episodes progress. Low-level winds do not share a common direction, however, as within-basin winds are strongly modulated by radiative effects and the location of the sounding with respect to the basin sidewalls. Yet, there is still a clear decoupling in speed and direction below the inversion top at all locations.

Consideration of a composite of observed 2-m temperature shows that, on average, VCPs have a temperature decrease at the beginnings that sometimes lasts until near the episode midpoint followed by a pronounced temperature increase at all locations (Fig. 4a). Note that the temperature evolution is similar regardless of the valley or basin size or location. Of the 29 episodes, 25 had this temperature pattern and an example is the 3–10 December 2006 event. The observed daily mean temperatures at the five locations for this event show that, roughly between 1 and 3 December, there are decreasing temperatures followed by steadily increasing temperatures between about 3 and 10 December (Fig. 4b). A within-basin warming is consistent with one type of idealized temperature evolution discussed in Whiteman et al. (1999; see their Fig. 10c). They argue that heat imbalances sometimes occur that lead to an increase in low-level temperatures. Increasing temperatures may be the result of a downward transport of heat due to mixing by intermittent turbulence or thermally driven flows (Whiteman et al. 2001). The fact that the majority of the cases have a similar pattern of evolution supports

the idea that synoptic forcing is key to VCP evolution most of the time. The remaining episodes have some basin-to-basin variability, such as the 22–30 October 2007 event. In this case, SLC and GJT have a net warming that is consistent with the composite (cf. Figs. 4a and 4c). The other locations have some warming initially, but then experience a temperature decrease near the midpoint of the event. Whiteman et al. (1999) argue this occurs when temperature changes above the cold pool are communicated to the cold pool itself, which also supports the notion that synoptic forcing is key to VCP evolution. [Consideration of observed midlevel temperatures does indeed show that midlevel temperatures at these locations do decrease during the latter half of this episode (not shown).]

b. Synoptic-scale evolution

The synoptic-scale flow patterns during VCPs are assessed using the Rapid Update Cycle (RUC; Benjamin 1989) model analyses. These analyses have a horizontal grid spacing of 13 km and 50 terrain-following vertical levels. Analyses are produced every hour from blending the 1-h forecast from the previous cycle with surface, aircraft, satellite, and upper-air measurements using the three-dimensional variational data analysis scheme. Composites of 500-hPa geopotential height, 700-hPa 24-h temperature tendency following the analysis time, sea level pressure, and virtual potential temperature (θ_v) from the lowest terrain-following level of the RUC analyses are used. [The RUC-diagnosed 2-m temperature does not consistently show good agreement with the observations; hence, the θ_v field from the lowest model level, whose patterns show a qualitatively better agreement with the observations (not shown), is used.]

Before the onset of a cold pool episode, there is typically a large trough over the western half of the United States (Fig. 5a) and cold air covers most of the western states (Fig. 5b). The cold-air surge likely accounts for the drop in the observed 2-m temperature that often occurs near the start of the episodes (Fig. 4a). At the start of the episodes, the western United States is beneath the ridge-to-trough segment of the upper-level wave and in a region of strong midlevel warming (Fig. 5c). There is also a large surface high pressure area over the western United States and cold pools are becoming evident in some basins and valleys (Fig. 5d). The middle period of the events is marked by a large upper-level ridge over the West Coast and moderate midlevel warming over the mountain states (Fig. 5e). Valley cold pools are also well defined in the θ_v analysis at this point and there is still a surface high pressure area over the western United States (Fig. 5f). At the ends of the epsiodes, the ridge amplitude is decreased and its axis is shifted eastward to over Wyoming, Colorado, and New Mexico (Fig. 5g). There is also a trough over the West Coast and strong midlevel cooling over the mountain states and the surface cold pools are not as well defined (Fig. 5h). After the episodes end, the trough has moved to over the mountain states, a new ridge is positioned along the west coast (Fig. 5i), and a new cold-air surge covers the western United States (Fig. 5j).

A more comprehensive view of the relationship between persistent VCP timing and upper-level wave patterns is provided in Fig. 6, which shows a timeline of the observed 500-hPa geopotential height from the BOI sounding. [Other sounding locations have similar patterns (not shown).] All of the episodes occur when there is an upper-level ridge and most VCPs only last as long as the ridge is present. In some episodes, such as from 15 to 21 January 2007, there is a short-lived decrease in the geopotential height near the middle of the episode. These decreases coincide with partial mix outs [see section 3c(3)].

Regardless of the length of the episode, the same progression of events is observed. This is demonstrated by using the 27–30 October 2006 and 15–25 November 2005 episodes. Both cases are preceded by a cold-air surge covering most of the mountain states (Figs. 7a and 7d) that appears to retreat to the east or northeast at the episode's onset (Figs. 7b and 7e), leaving behind pockets of low-θ_v air in the various basins and valleys by the episode midpoints (Figs. 7c and 7f). Aloft and at the start of each episode, there is an upper-level ridge near the west coast of the United States and midlevel warming over the mountain states (Figs. 8a and 8d). At the ends of these episodes, troughs are positioned near the West Coast and there is midlevel cooling over the mountain states (Figs. 8b and 8e). Observed soundings also agree closely with the composite soundings in Fig. 3, with significant midlevel warming at the episode onsets and strong midlevel cooling at the ends of the events (Figs. 8e and 8f).

c. Variations on the mean

Not every episode exactly fits the above-described patterns or sequence of events. Following are descriptions of episodes that vary from the mean. As is demonstrated below, although these cases do depart from the mean, synoptic-scale flow patterns still appear to dictate the evolution of VCPs.

1) REX BLOCKS

There is a small subset (eight) of episodes that have an upper-level wave pattern that is sometimes referred to as a Rex block or high-over-low block (Rex 1950). These blocks are characterized by a high pressure area positioned directly north of a low pressure area. A composite

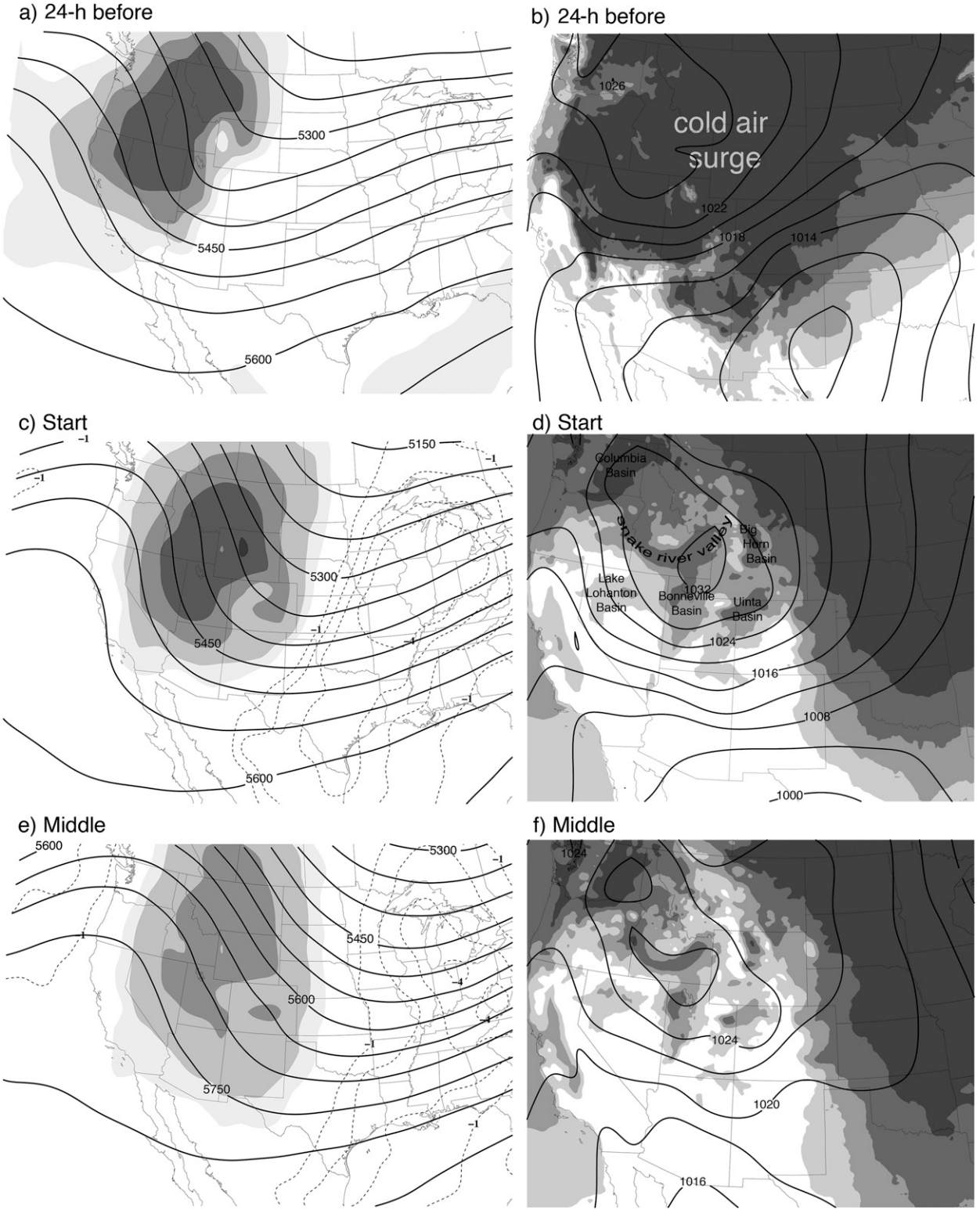

FIG. 5. Composite analyses of (left) 500-hPa geopotential height (m; solid contours) and 700-hPa 24-h temperature tendency (K; positive values are shaded and negative values are dashed contours) and (right) virtual potential temperature at the lowest model level (shaded) and sea level pressure (hPa; contoured). In this and all other similar figures, the temperature tendency is calculated over the 24-h period following the analysis times used in the composite of the geopotential height. The times shown are (a),(b) 24-h before the start of, (c),(d) at the start of, (e),(f) at the midpoint of, (g),(h) at the end of, and (i),(j) 24 h after the end of the episodes.

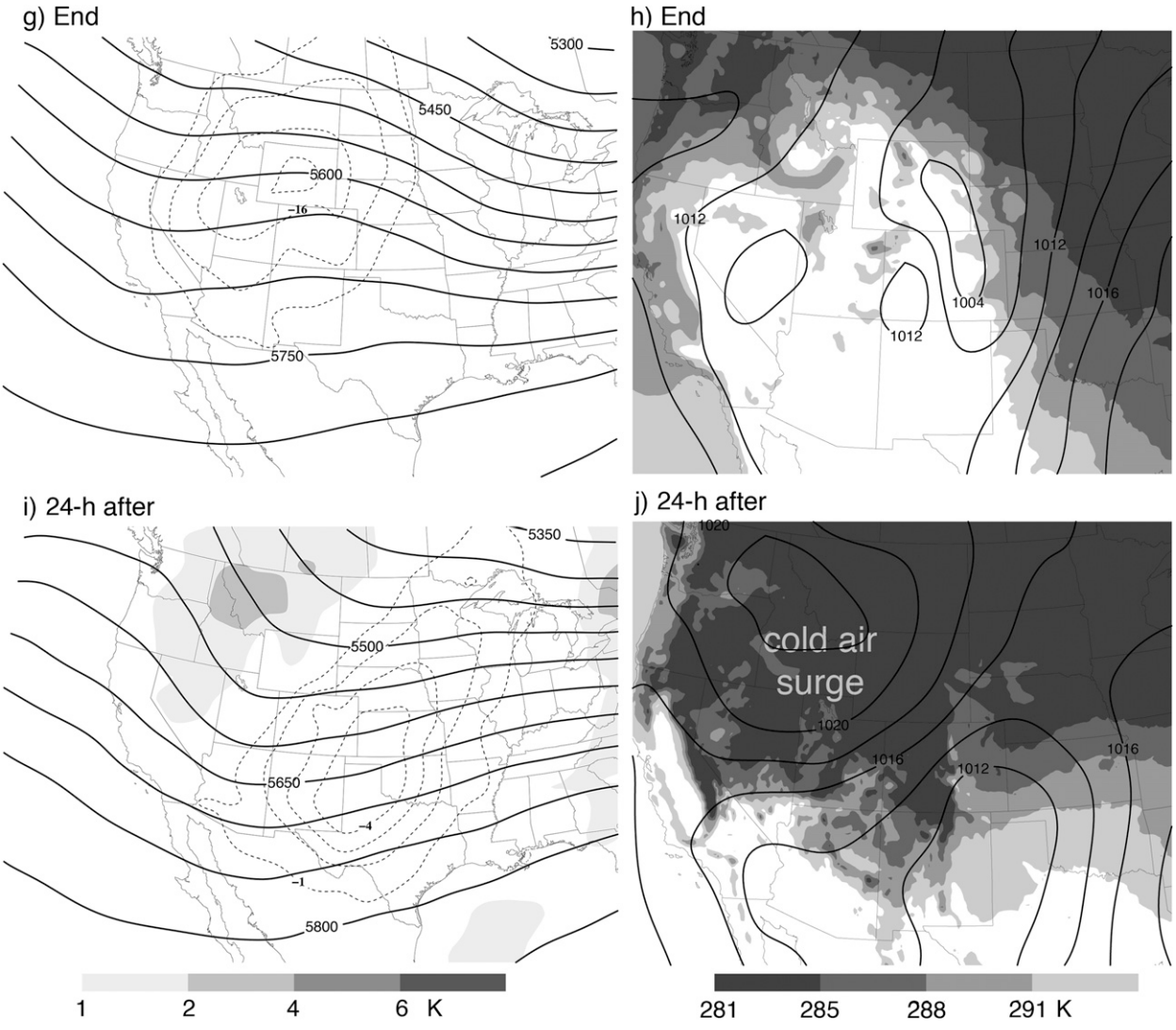

FIG. 5. (*Continued*)

of the 500-hPa geopotential height and 700-hPa 24-h temperature tendency at the start of these episodes shows that the high pressure lobe of the block and a well-defined region of midlevel warming are customarily over the western United States (Fig. 9a). (The reader may note that high pressure lobe is not directly north of the trough. This is because each episode has a slightly different position for the high and low pressure areas and because at the beginnings of the episodes, the blocking pattern is not completely established.) At the ends of these episodes, after the blocking pattern is removed, there is a weak ridge and strong midlevel cooling over the mountain states (Fig. 9b). These temperature tendency patterns are quite similar to those in Figs. 5c and 5g. A composite of soundings at SLC for Rex block episodes shows the ambient winds are not westerly, as they are in Fig. 3, but are initially from the southeast and switch to the west or southwest by the ends of the episodes. (The reader may note that the southeasterly winds in Fig. 9c are not consistent with the height contours in Fig. 9a. This is because there is a small cutoff low that is not captured given the contour spacing used in Fig. 9a.) However, the typical progression of temperature profiles is very similar to the composites in Fig. 3, with midlevel warming at the beginning and strong cooling at the end (Fig. 9c). Hence, this type of episode also appears to be primarily driven by the synoptic-scale wave evolution.

2) VARIATIONS AT THE ENDS OF VCPS

There is some variation in how VCP episodes end. Although the mechanisms of VCP removal are beyond

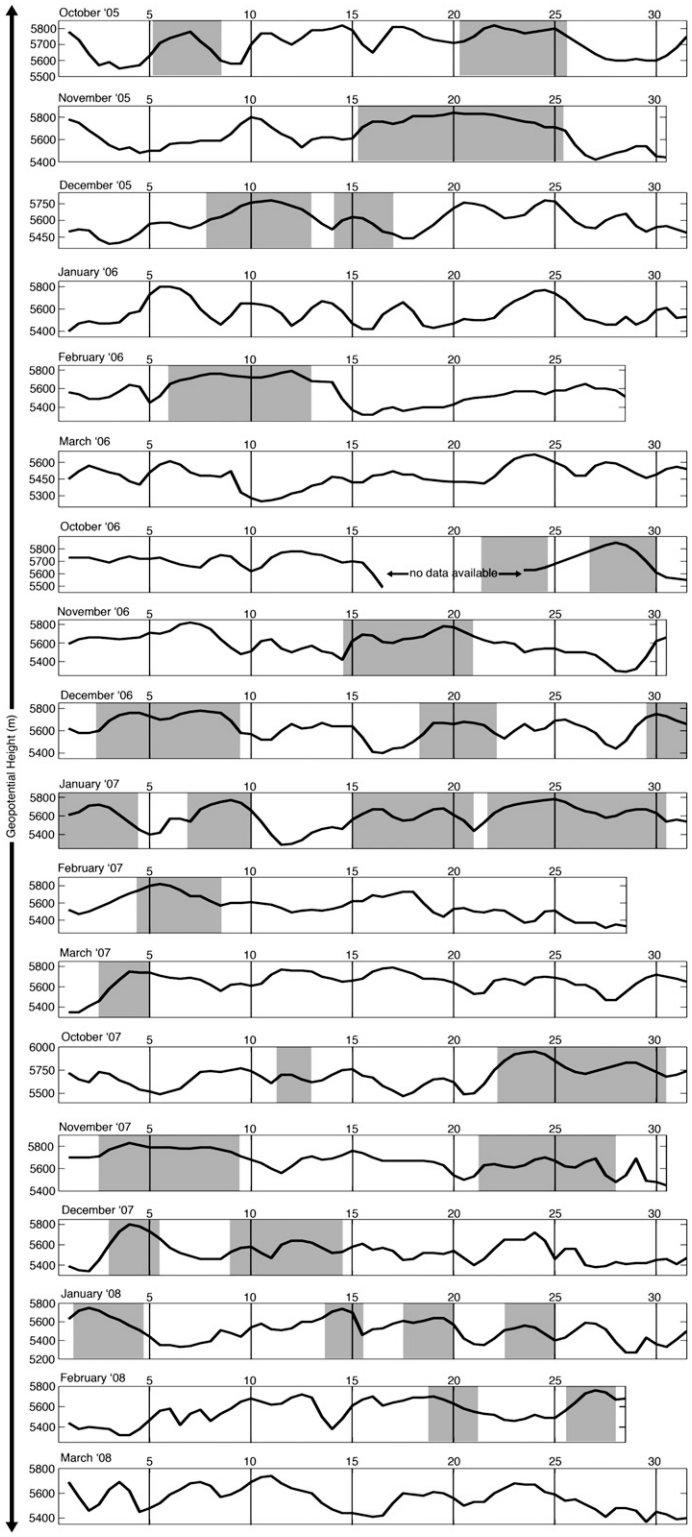

FIG. 6. A timeline of observed 500-hPa geopotential height at BOI from radiosonde data. The gray shading denotes times of VCP episodes. Sounding data were not available from 17 to 24 Oct 2006.

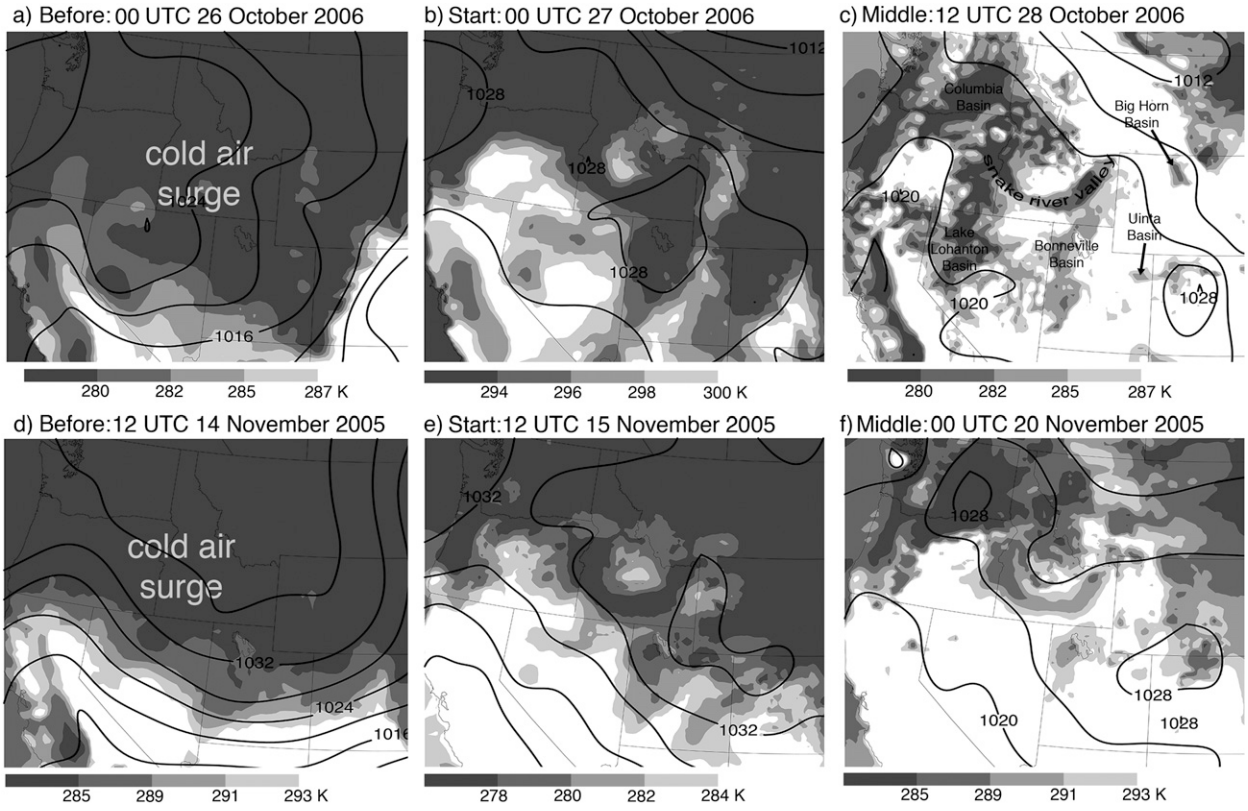

FIG. 7. The RUC-analyzed virtual potential temperature at the lowest model level (a),(d) 24 h prior to the start, (b),(e) at the start, and (c),(f) at the midpoint of the 27–30 Oct 2006 and 15–25 Nov 2005 episodes.

the scope of this research, it is possible that the means by which the cold pools are removed are case dependent. In some episodes (13), including the 15–21 January 2007 episode, there is a surface cold front. At 1200 UTC 20 January, a front is east and south of the Columbia River basin (Fig. 10a) and moves southeast, passing over the Bonneville Basin around 0000 UTC 21 January (Fig. 10b). By 1200 UTC 21 January, the front is east and south of the domain shown (Fig. 10c). The front may act to advect the VCPs out of the basins and valleys. Observed soundings at Salt Lake City for this event show strong cooling, with a temperature decrease of 10.4 K at 700 hPa (Fig. 11a). This event also has a deep, upper-level trough over the western United States and strong, localized cooling over the mountain states (Fig. 11b). All episodes with midlevel cooling in excess of about 8 K day^{-1} have a surface cold front.

The remaining 16 episodes have rather modest or weak midlevel cooling (less than about 8 K day^{-1}). Such an example is the 3–9 December 2006 event. Observed soundings at Salt Lake City at the end of this episode show a modest temperature decrease of 5.3 K at 700 hPa (Fig. 11c). The mid- and upper-level flows for this event have only a shallow, short-wave trough and widespread, weak, midlevel cooling (Fig. 11d). The passage of a short-wave trough typically leads to an increase in the crest-level wind speeds, which may lead to turbulent mixing and a top-down erosion of the cold pool (Petkovsek 1992; Vrhovec and Hrabar 1996; Zängl 2005b). The Salt Lake City sounding supports this notion as the soundings at 1200 UTC 9 December and 0000 UTC 10 December still have very shallow inversions near the surface (Fig. 11c). Composites of the flows for episodes with short-wave troughs but no surface cold front versus episodes with surface cold fronts are not provided because there is some case-to-case variation in the location of the upper-level trough and features of interest are smeared in the composites (not shown). Nevertheless, as Fig. 11 demonstrates, regardless of the method by which a VCP appears to be removed, either pattern is characterized by an approaching upper-level trough and midlevel cooling.

3) PARTIAL MIX OUTS

During some episodes, one or more station may cease to have a VCP toward the middle of the event, such as at BOI for the 15–21 January 2007 episode (Fig. 2). These temporary interruptions occur simultaneously with

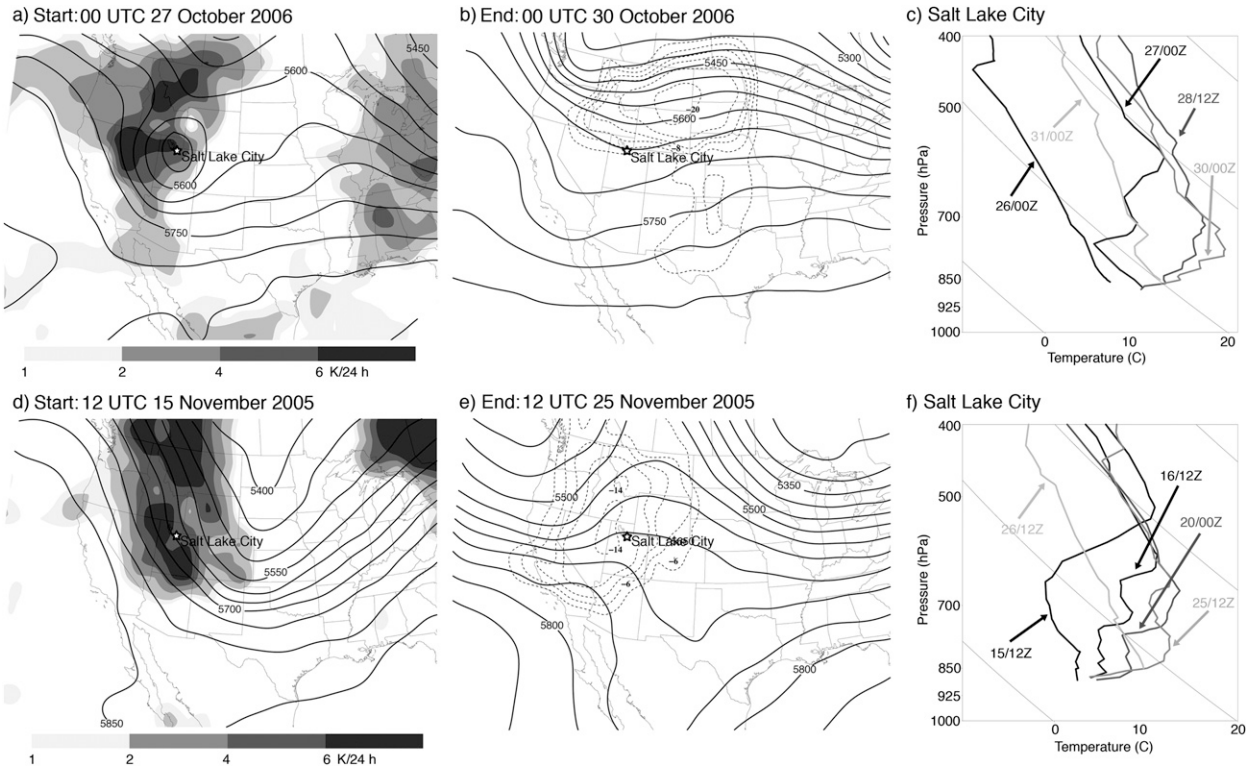

FIG. 8. (a),(b),(d),(e) The RUC-analyzed 500-hPa geopotential height (m; solid contours) and 700-hPa 24-h temperature tendency (K). In (a),(d), only positive values are shown and in (b),(e) only negative values are shown. (c),(f) The observed soundings at SLC. Times are denoted as dd/hhZ, where dd is the day and hh is the hour.

short-lived decreases in the geopotential height (Fig. 6). Wolyn and McKee (1989) and Whiteman et al. (1999) also observed this phenomenon. A time sequence of the RUC-analyzed geopotential height pattern for the 15–21 January 2007 event shows a Rex block over the western United States at 0000 UTC 16 January (Fig. 12a). At 0000 UTC 17 January, the high pressure lobe of this block has moved westward, over the Pacific Ocean, but it begins to move back onshore by 0000 UTC 18 January. Midlevel cooling is evident in the observed temperature profiles during this adjustment (shown in Figs. 12b with the SLC sounding). Before the partial mix out, there is midlevel warming and the inversion strengthens (16–17 January). The midlevels cool and the inversion weakens in response to the changes in the upper-level pattern (18 January). Afterward, the midlevels warm and the inversion restrengthens (20 January). The partial mix out is also evident through comparison of meteograms of observed 2-m temperatures at the basin and valley bottoms and tops. Traces for Salt Lake City and Alta, Utah, show that Alta has the warmer temperatures except during the partial mix out between 17 and 18 January (Fig. 12c). The pattern is much the same at Idaho Falls and Smiley Mountain: before and after the partial mix out, temperatures are higher at Smiley Mountain, but during the mix out, Idaho Falls has warmer temperatures (Fig. 12d). Even in the comparatively shallow and narrow Grand Valley, surface observations show evidence of a partial mix out as temperatures at Columbine Pass are warmer than at Montrose except during the mix out (Fig. 12e). Notice that the temperature patterns for locations in the bottoms of the basins and valleys are not affected by the partial mix out. Only locations that are outside of the valleys and basins are affected.

As the higher-elevation surface temperature traces in Figs. 12c–e indicate, the mid- and upper-level flow patterns provide guidance on whether the VCP has the potential to restrengthen (or reappear if it is removed during the mix out). Composites of the mid- and upper-level flow patterns at the beginnings and ends of the mix outs for the nine episodes with a partial mix out are provided in Figs. 13a and 13b, respectively. Note the moderate midlevel cooling (warming) at the beginnings (ends) of the mix outs. In fact, the flow patterns in Figs. 13a and 13b bear a remarkable similarity to those in Figs. 5e and 5c, respectively, except that the cooling in Fig. 13b is less than in Fig. 5e.

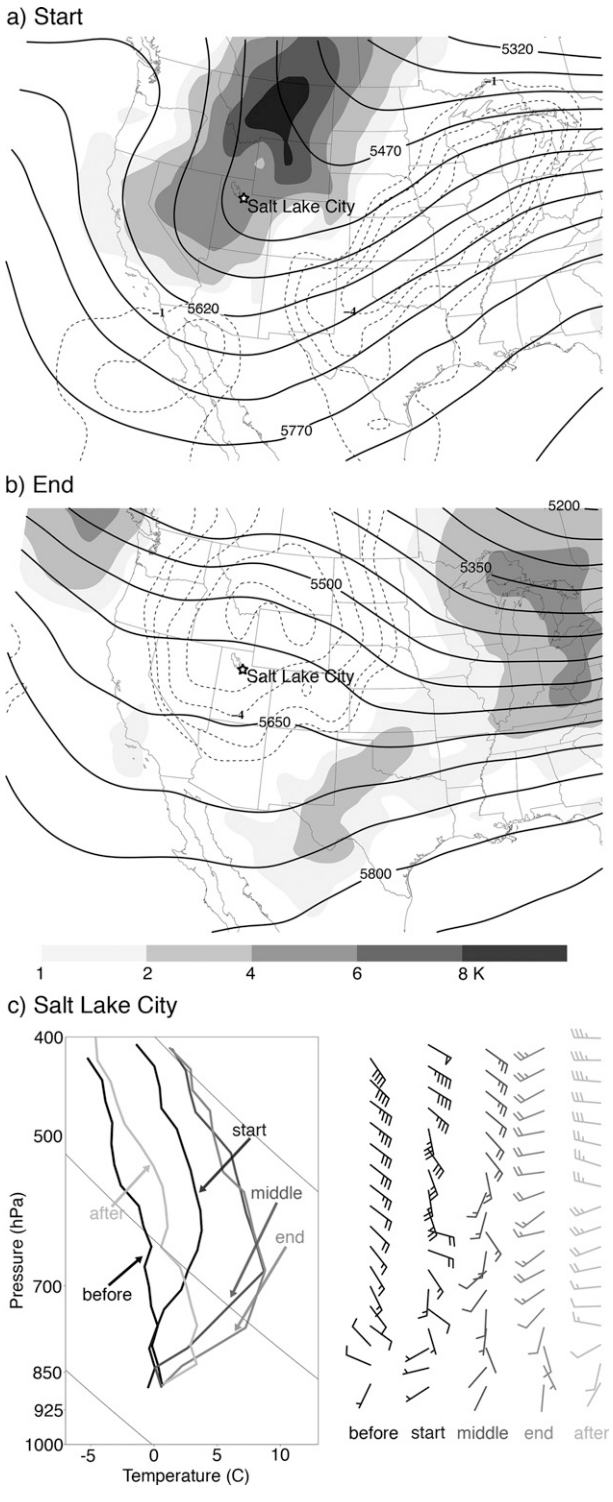

FIG. 9. Composite analyses of (a),(b) 500-hPa geopotential height (m; solid contours) and 700-hPa 24-h temperature tendency (K; positive values are shaded and negative values are dashed contours) and (c) observed soundings at SLC for VCP episodes occurring under a Rex block.

4. Nonepisodes and episodes with missing VCPs

Nonepisodic VCPs are those that do not occur simultaneously or nearly simultaneously with VCPs in two or more other valleys and basins from the five locations considered in Fig. 1. Nonepisodes share a number of similarities with episodic VCPs at mid- and upper levels, but have some differences near the surface.

A composite of all soundings for nonepisodic VCPs at key times in the VCP life cycle is provided in Fig. 14a. This composite includes soundings from all five locations. Because the elevations and surface pressures are different for each location, the geopotential heights are normalized such that the lowest height has an elevation of 0 m. The pressure levels are also normalized such that the lowest pressure is 925 hPa. The progression of temperature profiles in this composite agrees very well with the composites in Fig. 3 with a nearly moist-neutral profile before VCP onset, strong midlevel warming at VCP onset, and a continued warming and descent of the inversion top as time progresses. After the VCP ends, there is strong midlevel cooling. Low levels also have a progression that is similar to the composites in Fig. 3 and have some cooling at VCP onset followed by low-level warming. Finally, the winds are also similar to those in Fig. 3, starting with southwesterly flow that becomes more westerly as the VCPs end.

Composites of mid- and upper-level flow patterns at the starts and ends of nonepisodic VCPs are also similar to the episodes. At the starts, the mountain states are beneath the ridge-to-trough segment of the upper-level wave and beneath a region of strong midlevel warming (Fig. 14b). At the ends, there is strong midlevel cooling in association with an upper-level trough over the West Coast (Fig. 14c). These figures are very similar to the composites for the starts and ends of the episodes (Figs. 5c and 5e, respectively). Similar to the episodes, about three-quarters of the nonepisodes have a cold-air surge, but the surges usually do not extend as far west or south as in the episodes (not shown). Sometimes there is no cold-air surge, which may indicate that diabatic cooling is key to VCP formation for some of the nonepisodes.

There are five nonepisodes that do not fit the above-described pattern of synoptic flows. There is no one apparent explanation for why VCPs develop in these cases. Two of these nonepisodes occur in conjunction with precipitation and the soundings indicate the VCPs may be the product of strong evaporative cooling. (It is possible that the daytime inversions for these cases only coincidentally occur during a sounding time, but are not maintained during the entire 24-h period. Hence, these may not be true VCPs.) The other three nonepisodes may have formed from nocturnal cooling at night and

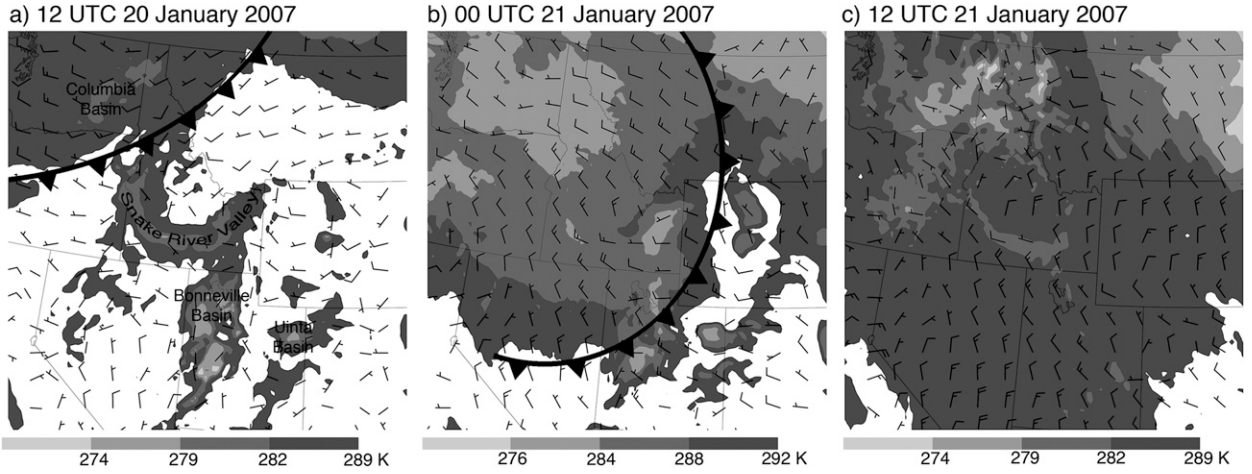

FIG. 10. The RUC analyses of virtual potential temperature at the lowest model level (shaded) and 10-m winds.

are maintained throughout the day by blocked or weakened insolation.

The nonepisodes, as well as episodes in which some basins and valleys do not have VCPs (or missing VCPs), present a special challenge to forecasters. What determines whether a valley or basin will have a VCP when the synoptic flow patterns are otherwise favorable? There are two reasons VCP criteria are not met: either the inversion is not maintained for 24 h, but the low-level winds are still weak enough (weak cases) or the low-level winds are too strong (strong cases). The weak (W) and strong (S) episodes are indicated in Fig. 2. A composite of the mid- and upper-level flows at the starts of the weak episodes shows the amplitude of the 500-hPa wave is weaker and the area of maximum warming is weaker and its center is farther north than in the composite of all episodes (cf. Figs. 15a and 5c). Six of the weak cases are missing VCPs at GJT and two are missing VCPs at REV. These two locations are farther south than the others, so the absence of VCPs may be due to seasonal effects. However, the Grand Valley is comparatively narrow and small, indicating basin geography may also play a role, with small, narrow basins being less likely to have a VCP when the synoptic forcing is weak. This is consistent with the claims of Whiteman et al. (1999). A composite at the start of the strong episodes shows a large-amplitude wave and very strong midlevel warming (Fig. 15b): a consequence of strong mid- and upper-level winds over the western United States. Without the benefits of sensitivity tests, we cannot conclusively determine why this pattern is not favorable for VCP formation at some locations. As is done for the episodes, nonepisodes can be partitioned as weak or strong. Figures showing this partition are not presented herein for the sake of brevity, but the patterns for these two types are very similar to those for the episodes (Figs. 15a and 15b) suggesting one could devise a set of thresholds to determine when VCP-producing criteria are optimized. However, our dataset is too small for meaningful thresholds to be obtained and this exercise is left for future research.

5. Conclusions

Previous studies of wintertime persistent valley cold pools indicate there may be a typical flow evolution at the synoptic scale that may dictate the formation, duration, and decay of persistent VCPs most of the time (Wolyn and McKee 1989; Savoie and McKee 1995; Mayr and McKee 1995; Whiteman et al. 1999, 2001; Zhong et al. 2001; Zängl 2005b). This possible connection is explored herein via a 3-yr climatology of persistent cold pools during winter in the western United States. Five valleys and basins of differing sizes, locations, and orientations are considered.

There are a number of clues that support the notion that persistent VCPs are strongly forced by synoptic-scale flow. These include the fact that most VCPs occur simultaneously or nearly simultaneously in multiple locations rather than as isolated events. A composite of the typical sounding progression indicates that all locations have a similar evolution, with strong midlevel warming (cooling) at VCP onset (demise). Conversely, low-level temperatures change only a small amount as the VCP evolves. The ambient wind direction is also similar during these events, with generally westerly or west-southwesterly flow above the valley or basin. The typical surface temperature evolution consists of initially decreasing temperatures followed by a steady increase. These findings hold for both large and small

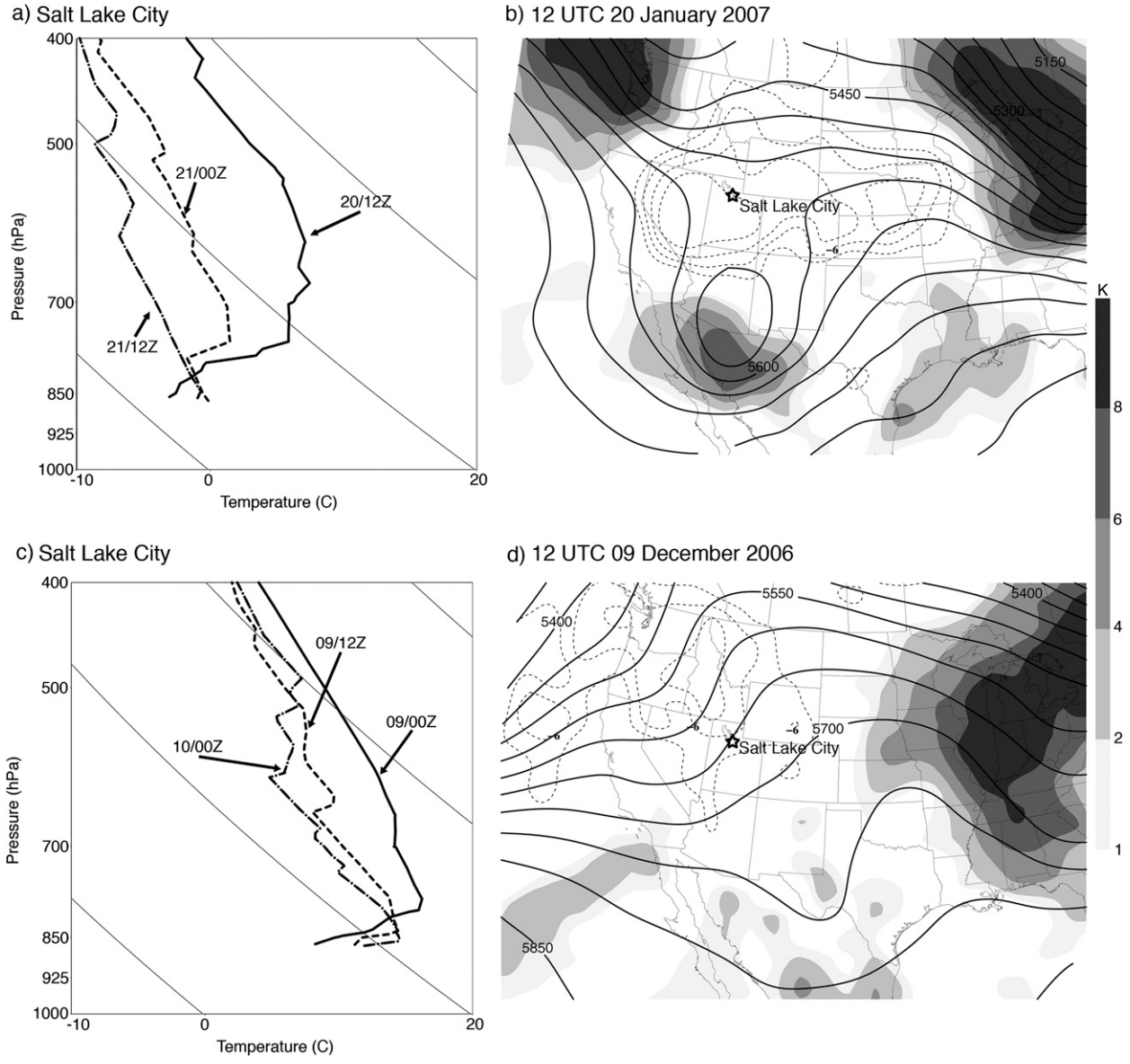

FIG. 11. The (a),(c) observed soundings at SLC and (b),(d) RUC-analyzed 500-hPa geopotential height (m; solid contours) and 700-hPa 24-h temperature tendency (K; positive values are shaded and negative values are dashed contours) at the ends of the (top) 15–21 Jan 2007 and (bottom) 3–9 Dec 2006 episodes.

basins and valleys and regardless of the location or complexity of the basin or valley.

Consideration of the prevalent large-scale flow patterns during VCP episodes (times when three or more locations have persistent VCPs) shows the episode starts often coincide with strong midlevel warming that is associated with an approaching upper-level, large-amplitude ridge. In every case, the episodes last as long as the ridge remains over the western United States. Episodes usually end with an approaching upper-level trough and as the western United States is beneath an area of midlevel cooling. This synoptic-scale flow progression is consistent with previous case studies of persistent wintertime cold pools (Wolyn and McKee 1989; Whiteman et al. 1999, 2001; Zhong et al. 2001; Zängl 2005b).

There are some variations from the typical flow patterns that are worthy of note. Some episodes occur under a Rex block, but these cases still have an upper-level high pressure area and strong midlevel warming over the western United States at VCP onset and a temperature profile evolution that is similar to the composites for all cases. Some of the episodes end with a surface cold front while others have no front, but only an upper-level short-wave trough. The mechanics of

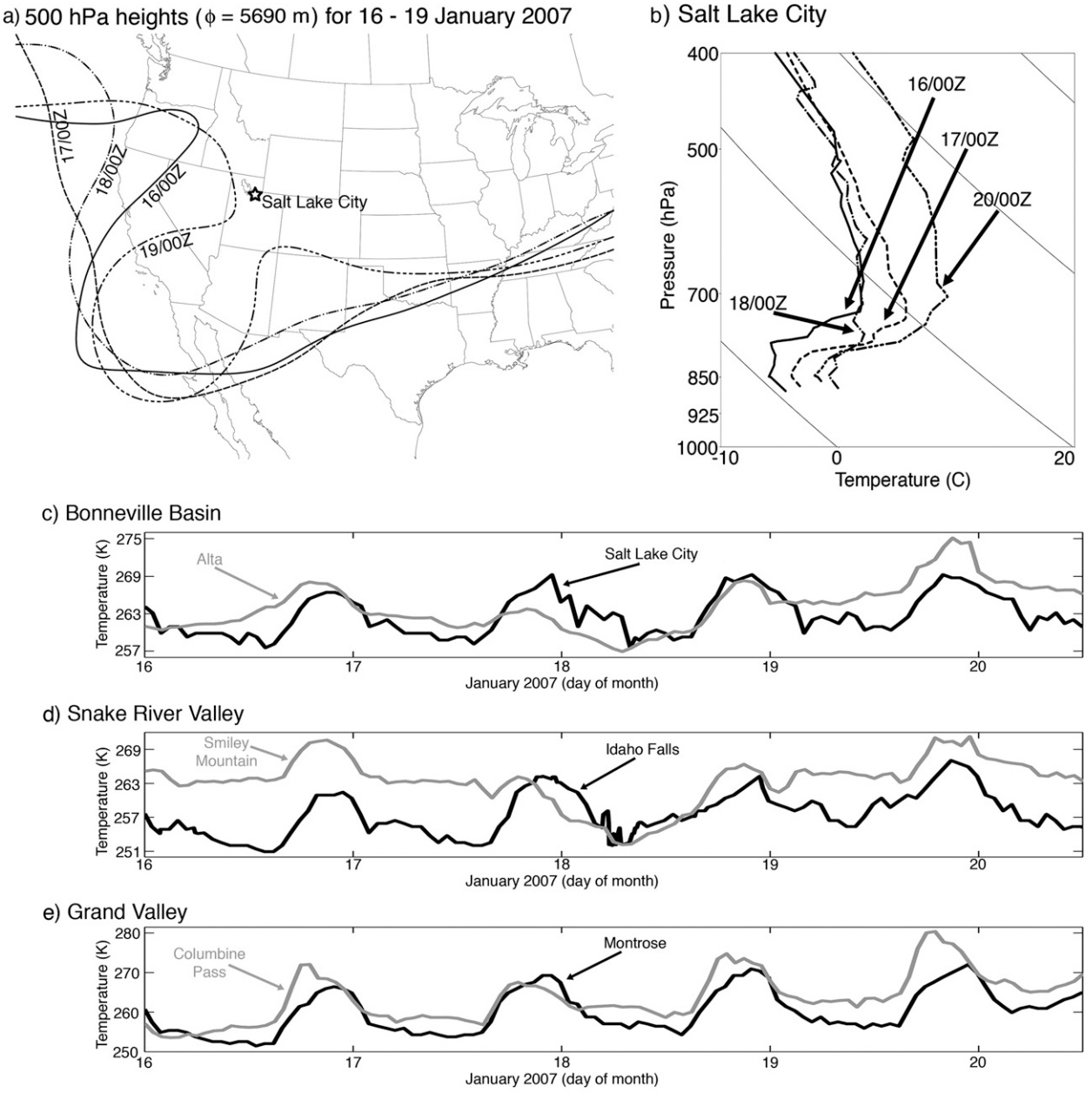

FIG. 12. The (a) RUC analyses of a time sequence of 500-hPa geopotential heights, (b) observed soundings at SLC, and observed 2-m temperature at (c) SLC and Alta (elevations of 1288 and 3372, respectively), (d) Idaho Falls and Smiley Mountain (elevations of 1435 and 2901 m, respectively), (e) Montrose and Columbine Pass (elevations of 1755 and 2865 m, respectively). In (c)–(e) the day markers indicate 0000 UTC of the day given.

VCP removal may be different for these two patterns, with some cold pools appearing to be removed via advection and others by turbulent erosion. Some of the episodes have partial mix outs toward their midpoints. A partial mix out is a time when the VCP criteria are not strictly met at all locations or the VCP is temporarily weakened but regains its strength in a short period of time. In every case with a partial mix out, the mix out can be directly attributed to short-lived changes (i.e., a reduction in the ridge amplitude or the passage of a weak trough) in the synoptic-scale flow pattern. Midlevel cooling occurs coincident with the weakening of the VCP inversion, and midlevel warming occurs as the VCP regains its strength. These cooling and warming patterns are similar to those at episode ends and beginnings.

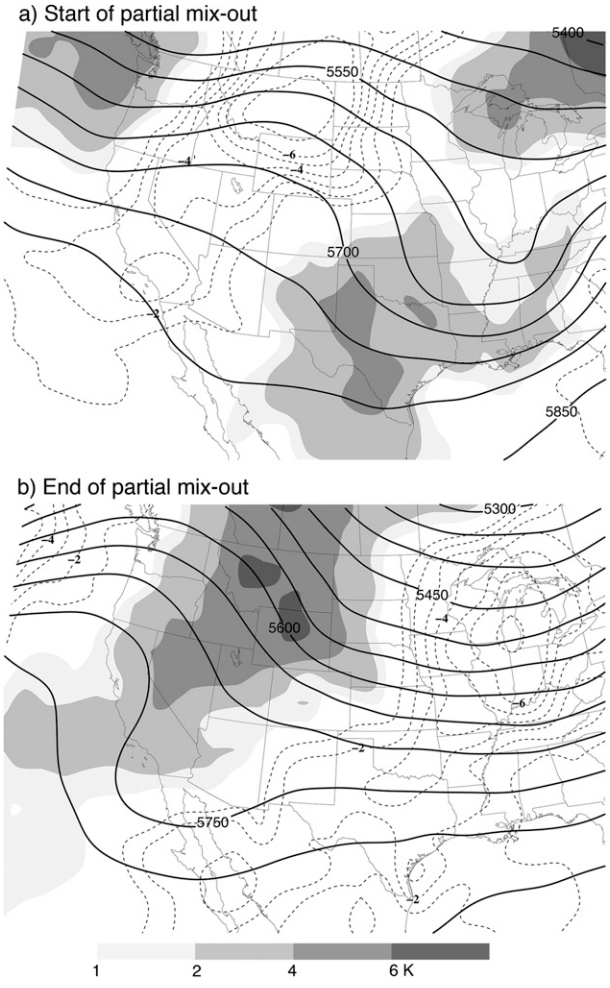

FIG. 13. Composites of the RUC-analyzed 500-hPa geopotential height (m; solid contours) and 700-hPa 24-h temperature tendency (K; positive values are shaded and negative values are dashed contours) for (a) starts of and (b) ends of partial mix outs.

Nonepisodic VCPs are also considered. A composite of nonepisodic soundings shows that the temperature profiles are very similar to those for the episodes, with strong midlevel warming (cooling) at VCP onset (demise). Low-level temperatures experience only a slight warming during nonepisodes. Nonepisodes usually start as an upper-level ridge and its associated area of midlevel warming moves over the western states, similar to the start of an episode. The nonepisode ends usually coincide with the passage of an upper-level trough and its associated area of midlevel cooling, similar to the end of an episode. Although some nonepisodes have a low-level cold-air surge, the surges usually do not extend as far west or south as in the episodes.

In summary, regardless of whether the VCP was a part of an episode or a nonepisode, regardless of whether the VCP was at a higher or more southerly latitude,

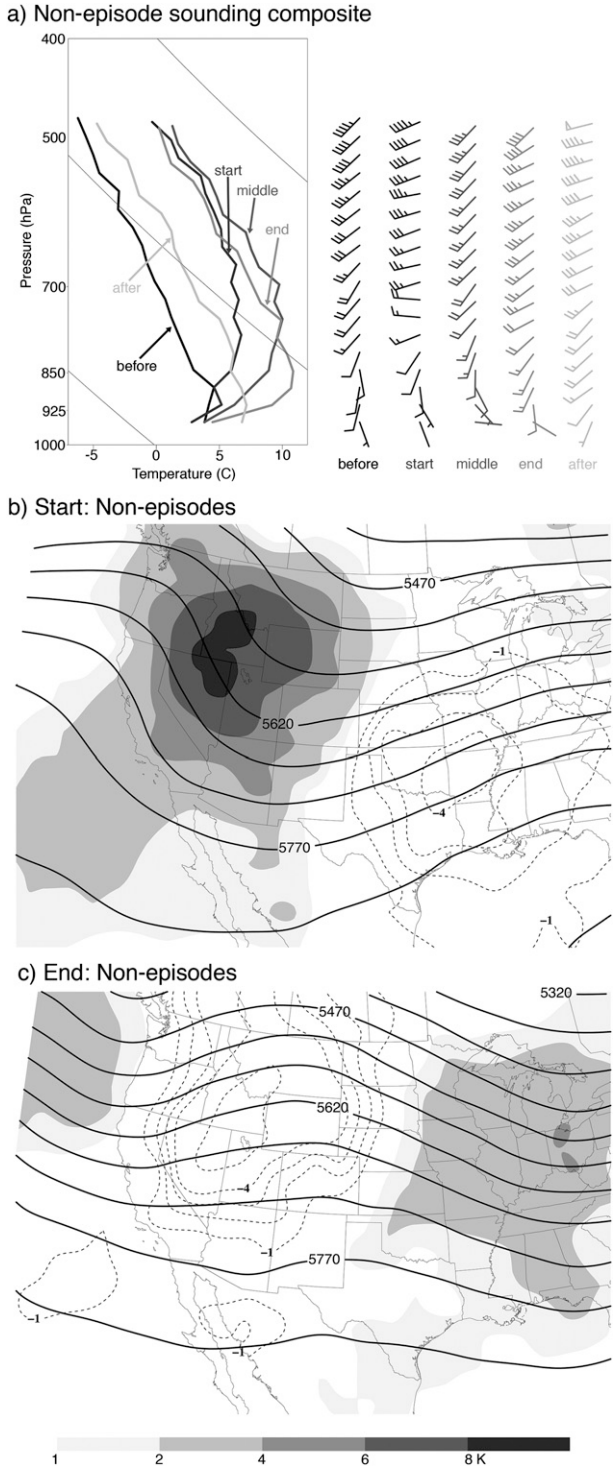

FIG. 14. Composites of (a) observed soundings (at all locations) and (b),(c) RUC-analyzed 500-hPa geopotential height (m; solid contours) and 700-hPa 24-h temperature tendency (K; positive values are shaded and negative values are dashed contours). In (a), the soundings have been normalized to a surface elevation of 0 m and surface pressure of 925 hPa.

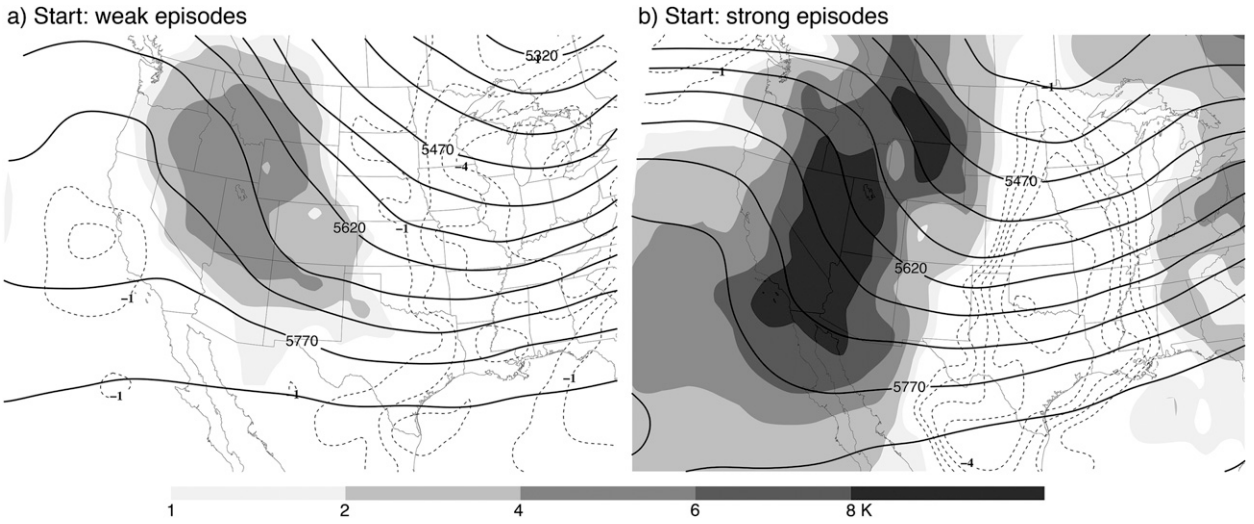

FIG. 15. Composites of the RUC-analyzed 500-hPa geopotential height (m; solid contours) and 700-hPa 24-h temperature tendency (K; positive values are shaded and negative values are dashed contours) for VCP episodes where one or more stations does not have a VCP due to (a) a weak upper-level forcing or (b) upper-level winds that are too strong.

regardless of whether in a valley or basin, and regardless of whether the valley or basin is large (such as the Columbia River basin) or narrow (like the Grand Valley), *almost all VCPs experience the above-described sequence of synoptic-scale flow patterns*. Presuming the synoptic-scale wave evolution is accurately captured in numerical weather prediction models, then, forecasters may be able to use the wave motions and related midlevel temperature changes to anticipate VCP formation and demise, particularly in basins and valleys where surface and upper-air observations are not very dense or reliable.

There are a few caveats to be mentioned before closing. First is the issue of midlevel warming and cooling. Temperature tendencies shown herein are total tendencies and, hence, include changes due to horizontal advection, subsidence or ascent, diabatic effects, etc. The individual contributions of these effects to midlevel temperature changes still need to be quantified. Second, diabatic effects at the surface, such as reduced radiation from snow cover or clouds, have not been considered. It is possible that some of the VCPs in our collection would not have existed were they not enhanced by diabatic effects. This is an important consideration for forecasting and numerical modeling.

Acknowledgments. This research was supported by the National Research Council and the National Severe Storms Laboratory. The RUC model data were provided by the National Center for Atmospheric Research. The surface observations were provided by the University of Utah Mesowest. Radiosonde data were provided by the University of Wyoming. Conversations with D. M. Schultz helped guide the direction of this research. Comments by two anonymous reviewers were very helpful for improving the text.

REFERENCES

Bader, D. C., and T. B. McKee, 1985: Effect of shear, stability and valley characteristics on the destruction of temperature inversions. *J. Climate Appl. Meteor.,* **24,** 822–832.

Banta, R., and W. R. Cotton, 1981: An analysis of the structure of local wind systems in a broad mountain basin. *J. Appl. Meteor.,* **20,** 1255–1266.

Benjamin, S. G., 1989: An isentropic mesoα-scale analysis system and its sensitivity to aircraft and surface observations. *Mon. Wea. Rev.,* **117,** 1586–1603.

Billings, B. J., V. Grubišić, and R. D. Borys, 2006: Maintenance of a mountain valley cold pool: A numerical study. *Mon. Wea. Rev.,* **134,** 2266–2278.

Cheng, W. Y. Y., and W. J. Steenburgh, 2007: Strengths and weaknesses of MOS, running-mean bias removal, and Kalman filter techniques for improving model forecasts over the western United States. *Wea. Forecasting,* **22,** 1304–1318.

Fast, J. D., S. Zhong, and C. D. Whiteman, 1996: Boundary layer evolution within a canyonland basin. Part II: Numerical simulations of nocturnal flows and heat budgets. *J. Appl. Meteor.,* **35,** 2162–2178.

Hart, K. A., W. J. Steenburgh, D. J. Onton, and A. J. Siffert, 2004: An evaluation of mesoscale-model-based model output statistics (MOS) during the 2002 Olympic and Paralympic Winter Games. *Wea. Forecasting,* **19,** 200–218.

——, ——, and ——, 2005: Model forecast improvements with decreased horizontal grid spacing over finescale intermountain orography during the 2002 Olympic Winter Games. *Wea. Forecasting,* **20,** 558–576.

Hill, C. D., 1993: Forecast problems in the western region of the National Weather Service: An overview. *Wea. Forecasting,* **8,** 158–165.

Hoggarth, A. M., H. D. Reeves, and Y.-L. Lin, 2006: Formation and maintenance mechanisms of the stable layer over the Po Valley during MAP IOP-8. *Mon. Wea. Rev.,* **134,** 3336–3354.

Lee, T. J., R. A. Pielke, R. C. Kessler, and J. Weaver, 1989: Influence of cold pools downstream of mountain barriers on downslope winds and flushing. *Mon. Wea. Rev.,* **117,** 2041–2058.

Lenschow, D. H., B. B. Stankov, and L. Mahrt, 1979: The rapid morning boundary-layer transition. *J. Atmos. Sci.,* **36,** 2108–2124.

Mayr, G. J., and T. B. McKee, 1995: Observations of the evolution of orogenic blocking. *Mon. Wea. Rev.,* **123,** 1447–1464.

Pataki, D. E., B. J. Tyler, R. E. Peterson, A. P. Nair, W. J. Steenburgh, and E. R. Pardyjak, 2005: Can carbon dioxide be used as a tracer of urban atmospheric transport? *J. Geophys. Res.,* **110,** D15102, doi:10.1029/2004JD005723.

Petkovsek, Z., 1992: Turbulent dissipation of cold air like in a basin. *Meteor. Atmos. Phys.,* **47,** 237–245.

Reeves, H. D., and Y.-L. Lin, 2006: Effect of stable layer formation over the Po Valley on the development of convection during MAP IOP-8. *J. Atmos. Sci.,* **63,** 2567–2584.

Rex, D. F., 1950: Blocking action in the middle troposphere and its effect upon regional climate. Part I: An aerological study of blocking action. *Tellus,* **2,** 275–301.

Savoie, M. H., and T. B. McKee, 1995: The role of wintertime radiation in maintaining and destroying stable layers. *Theor. Appl. Climatol.,* **52,** 43–54.

Smith, R., and Coauthors, 1997: Local and remote effects of mountains on weather: Research needs and opportunities. *Bull. Amer. Meteor. Soc.,* **78,** 877–892.

Struthwolf, M., 2005: An evaluation of fog forecasting tools for a fog event and non-event at Salt Lake City International Airport. NWS Tech. Attach. 05-05, 24 pp. [Available online at http://www.wrh.noaa.gov/wrh/05TAs/ta0505.pdf.]

Vrhovec, T., 1991: A cold air lake formation in a basin: A simulation with a mesoscale numerical model. *Meteor. Atmos. Phys.,* **8,** 91–99.

——, and A. Hrabar, 1996: Numerical simulations of dissipation of dry temperature inversions in basins. *Geofizika,* **13,** 81–96.

Whiteman, C. D., 1982: Breakup of temperature inversions in deep mountain valleys: Part I. Observations. *J. Appl. Meteor.,* **21,** 270–289.

——, and T. B. McKee, 1982: Breakup of temperature inversions in deep mountain valleys: Part II. Thermodynamic model. *J. Appl. Meteor.,* **21,** 290–302.

——, X. Bian, and S. Zhong, 1999: Wintertime evolution of the temperature inversion in the Colorado Plateau basin. *J. Appl. Meteor.,* **38,** 1103–1117.

——, S. Zhong, W. J. Shaw, J. M. Hubbe, X. Bian, and J. Mittelstadt, 2001: Cold pools in the Columbia Basin. *Wea. Forecasting,* **16,** 432–447.

Wolyn, P. G., and T. B. McKee, 1989: Deep stable layers in the intermountain western United States. *Mon. Wea. Rev.,* **117,** 461–472.

Zängl, G., 2002: Improved method for computing horizontal diffusion in a sigma-coordinate model and its application to simulations over mountainous topography. *Mon. Wea. Rev.,* **130,** 1423–1432.

——, 2003: The impact of upstream blocking, drainage flow, and the geostrophic pressure gradient on the persistence of cold-air pools. *Quart. J. Roy. Meteor. Soc.,* **129,** 117–137.

——, 2005a: Formation of extreme cold-air pools in elevated sinkholes: An idealized numerical process study. *Mon. Wea. Rev.,* **133,** 925–941.

——, 2005b: Wintertime cold-air pools in the Bavarian Danube Valley basin: Data analysis and idealized numerical simulations. *J. Appl. Meteor.,* **44,** 1950–1971.

Zhong, S., C. D. Whiteman, X. Bian, W. J. Shaw, and J. M. Hubbe, 2001: Meteorological processes affecting the evolution of a wintertime cold air pool in the Columbia Basin. *Mon. Wea. Rev.,* **129,** 2600–2613.